



Mechanisms and Optimization Design of Flow-Induced Vibration Energy Harvesting: A Review

Jinshuai Liu¹, Xingrong Huang¹ and Zhe Li^{2,*}

¹Sino-French Carbon Neutrality Research Center, École Centrale de Pékin, Beihang University, Beijing 100191, China

²LHEEA Lab, Nantes Université, École Centrale de Nantes, CNRS, Nantes, France

Abstract

With the widespread deployment of the Internet of Things (IoT) and distributed sensing networks in marine and industrial environments, energy harvesting based on Flow-Induced Vibration (FIV) has garnered significant attention due to its high energy density and environmental adaptability. This paper provides a comprehensive review of the evolution of FIV energy harvesting systems, with a particular focus on absorber-based configurations. First, the classification of existing systems is systematically outlined, and the theoretical foundations of the classic linear Tuned Mass Damper (TMD) are revisited. The review critically analyzes the inherent limitations of linear theories, specifically frequency detuning and high mass dependency, when applied to complex, variable-frequency flow fields. Subsequently, the paper synthesizes the paradigm shift in system design, highlighting three core evolutionary paths: (1) Stiffness nonlinearity: The transition from linear resonance to Nonlinear Energy Sinks (NES) and bistable mechanisms to achieve broadband energy capture; (2) Mass

decoupling: The shift from reliance on physical mass to inertial amplification (Inerter/TMDI) to achieve lightweight designs; and (3) Flow field reconstruction: The progression from passive adaptation to source enhancement via Passive Turbulence Control (PTC) and wake interference. Finally, the paper summarizes current technical challenges and offers perspectives on future research directions, including Fluid Mechanics, Bionics, Computer Science, Materials Science.

Keywords: flow-induced vibration (FIV), energy harvesting, nonlinear energy sink (NES), inerter, passive turbulence control (PTC).

Abbreviations

CFD	Computational Fluid Dynamics
DES	Detached Eddy Simulation
DOF	Degree-of-Freedom
EBEH	Electromagnetic Bi-stable Harvester
ECP	Energy Concentration Pipe
FIV	Flow-Induced Vibration
LES	Large Eddy Simulation
NES	Nonlinear Energy Sink
PTC	Passive Turbulence Control
PTO	Power Take-Off
TET	Targeted Energy Transfer
TMD	Tuned Mass Damper
TMDI	Tuned Mass Damper Inerter
VIV	Vortex-Induced Vibration



Submitted: 03 March 2026

Accepted: 13 April 2026

Published: 18 April 2026

Vol. 1, No. 1, 2026.

10.62762/JCN.2026.299279

*Corresponding author:

✉ Zhe Li

zhe.li@ec-nantes.fr

Citation

Liu, J., Huang, X., & Li, Z. (2026). Mechanisms and Optimization Design of Flow-Induced Vibration Energy Harvesting: A Review. *Journal of Carbon Neutrality*, 1(1), 10–28.



© 2026 by the Authors. Published by Institute of Central Computation and Knowledge. This is an open access article under the CC BY license (<https://creativecommons.org/licenses/by/4.0/>).

Symbols

A_y	Transverse vibration amplitude
b	Inertance
C_D, C_{L0}	Drag and lift coefficients
D, L	Cylinder diameter and length
f_s, ω_n	Vortex shedding and natural frequencies
F_{VIV}	Vortex-induced force
k_1, c_1, m_1	Primary system parameters
k_2, c_2, m_2	Absorber parameters
k_N	NES nonlinear stiffness
m^*	Mass ratio
Re, St	Reynolds and Strouhal numbers
U, U_∞	Flow velocity
β_{fit}, ζ	Damping ratios
η	Energy extraction efficiency
θ	Rotational / Inertance angle
ρ	Fluid density

1 Introduction

1.1 Global Energy Transition and the Dual Carbon Strategy Context

Currently, the global energy structure is in a critical window of transition. Despite continuous growth in clean energy investments, fossil fuels still dominate, making the carbon reduction mission arduous [1]. To fulfill the *Paris Agreement*, China has explicitly proposed the Dual Carbon strategic goal and outlined ambitious non-fossil energy consumption targets in its national development plans [2–4]. In this context, marine fluid energy serves not only as a core technology supporting the 'Smart Ocean' strategy but also as a crucial breakthrough point for cultivating New Quality Productive Forces in the energy sector [5].

1.2 Unique Advantages and Physical Characteristics of Fluid Energy (Blue Energy)

Marine fluid energy possesses significant advantages, such as high energy density and widespread distribution [6]. From a physical perspective, water flow contains far more energy than wind energy for the same cross-sectional area. According to the fluid power equation:

$$P = \frac{1}{2} \rho A v^3 \quad (1)$$

where ρ is the fluid density, A is the cross-sectional area, and v is the flow velocity. Because the density of water is approximately 800 times that of air, marine fluid energy exhibits extremely high power density [7]. Even in low-flow-speed environments (< 1 m/s), it

retains high harvesting value, making it critical for supporting national energy security and the "Blue Territory" strategy.

1.3 Energy Bottlenecks in Smart Ocean Sensing Networks

With the exponential growth of distributed Wireless Sensor Networks (WSN) in deep-sea exploration and marine monitoring [8], the energy supply for these peripheral nodes has become a critical bottleneck:

- **Lifespan and Environmental Constraints of Power Sources:** Currently, underwater nodes rely predominantly on lithium batteries, which face severe limitations. In extreme deep-sea environments (high salinity, high pressure, extreme cold), the charge migration rate and encapsulation reliability of chemical batteries drop significantly [9]. Furthermore, the prohibitive operational and maintenance costs of battery replacement completely fail to match the 10-year+ service life cycle of marine equipment [10].
- **System Lightweighting and Structural Compatibility:** For long-endurance drones or deep-sea submerged buoys, traditional rotary power generation devices add excessive payload and drag. Utilizing Flow-Induced Vibration (FIV) principles—such as Vortex-Induced Vibration (VIV), Flutter, or Galloping—enables lightweight, self-starting, and low-load energy harvesting. This makes FIV the optimal pathway for achieving self-sustained system operation in distributed sensing networks.

1.4 Literature Search Strategy and Review Scope

To ensure a comprehensive and transparent analysis of recent advancements in this field, a systematic literature search was conducted. The retrieval spans prominent databases, including Web of Science, Scopus, ScienceDirect, ASME Digital Collection, and IEEE Xplore, focusing on the contemporary trajectory from 2020 to 2025. The retrieval strategy employed Boolean combinations of keywords across three domains: vibration suppression mechanisms, energy harvesting paradigms, and structural optimization. This review explicitly focuses on absorber-based configurations driven by their unique dual functionality: they act as both vibration mitigators and highly efficient energy concentrators. By integrating nonlinear stiffness, inertial decoupling, and passive flow control, these systems uniquely address the inherent

narrow-band and mass-dependency bottlenecks of classic linear theories, representing the most promising evolutionary path for fluid energy harvesting.

2 Significance of Research and Engineering Application Value

Research on Flow-Induced Vibration (FIV) energy harvesting technology is not only crucial for solving engineering challenges related to distributed marine energy supply but also possesses profound theoretical innovation value and significant ecological benefits.

2.1 Enhancing Equipment Self-Sustainment

By converting ambient fluid kinetic energy into electricity, marine monitoring equipment can transition from battery-limited lifespans to real-time, all-weather operation. This self-powered approach addresses the limitations of traditional observation platforms that typically require annual maintenance [11]. By extending the operation and maintenance (O&M) cycle to a decadal scale (5–10 years), the comprehensive life-cycle costs can be reduced by over 60% [12].

2.2 Theoretical Breakthroughs

Fluid energy harvesting involves complex Fluid-Structure Interaction (FSI) phenomena. Current research focuses on utilizing nonlinear bistable or multi-stable characteristics to overcome the narrow bandwidth limitations of traditional linear systems, achieving broadband responses to variable ocean currents. The exploration of fluid energy harvesting systems helps overcome theoretical bottlenecks in "Fluid-Structure-Electric" multi-field coupling, providing core theoretical support for designing highly robust and efficient distributed energy harvesters [13].

2.3 Environmental Benefits

Traditional lithium batteries face risks of encapsulation failure in deep-sea high-pressure and highly corrosive environments [14]. Once leakage occurs, toxic electrolytes and heavy metals will directly enter the marine ecological cycle, causing irreversible biological toxicity [15]. Fluid energy harvesters mostly employ eco-friendly smart materials, effectively alleviating the pressure of electronic waste accumulation in ecologically sensitive areas.

3 Complexity of the Fluid Environment and Energy Harvesting Challenges

Although fluid kinetic energy holds immense potential, its highly complex spatiotemporal environment poses severe challenges to the structural robustness, frequency matching, and energy conversion efficiency of harvesters.

3.1 Spatial Multidimensionality

Real marine flow fields exhibit significant multi-directional and transient characteristics. Unlike ideal unidirectional flows, ocean currents often feature rotating or reciprocating vectors due to complex bathymetry and oceanographic dynamics. These sudden shifts in flow direction cause massive off-axis load fluctuations, severely diminishing the energy capture efficiency of traditional single-degree-of-freedom (1-DOF) harvesters [16].

3.2 Unsteady Flow and Large-Period Disturbances

Fluid kinetic energy input is highly pulsatile. Extreme oceanic events, such as internal solitary waves, can trigger sudden and destructive surges in instantaneous flow velocity [17]. These high-intensity disturbances require the harvesting system to possess not only broadband capture capabilities but also extreme structural load tolerance to prevent catastrophic failure [18].

3.3 Turbulence-Induced Decoherence

In practical engineering conditions, multi-scale irregular vortices create a highly turbulent environment that severely degrades the dynamic response of FIV systems. High turbulence intensity disrupts the coherence of vortex shedding, leading to "lock-in" region drift and random amplitude fluctuations [19]. Consequently, stable periodic vibrations degrade into chaotic or narrowband random responses, potentially reducing the energy conversion efficiency of VIV devices by 30%–50% compared to ideal laminar conditions [20].

4 Linear Fluid Energy Harvesting: Configuration Evolution, Parameter Optimization, and Inherent Limitations

Although traditional horizontal or vertical axis turbines are technologically mature in large-scale hydropower projects (e.g., the Three Gorges turbine units), rotating machinery in distributed marine sensing power supplies faces issues such as high mechanical friction losses, complex sealing structures,

and excessive component size [21]. Furthermore, the attachment of marine organisms (e.g., barnacles, algae) can significantly alter blade configurations, disrupting hydraulic balance. Additionally, rotating devices typically have a distinct "cut-in speed" threshold, making it difficult to capture weak kinetic energy widespread in the ocean (flow velocity < 0.5 m/s) [22].

In contrast, energy harvesting technology based on FIV offers significant advantages: firstly, the structure is simplified, eliminating the need for complex speed-increasing gearboxes and rotary seals, making it easier to achieve solid-state encapsulation; secondly, vibration-based devices are more sensitive to weak flow fields and can induce resonance at extremely low Reynolds numbers through reasonable stiffness design [20]. However, single-degree-of-freedom FIV harvesting devices (Figure 1) often exhibit narrow lock-in ranges and insufficient structural robustness when facing the aforementioned complex and random flow environments. To further improve system adaptability to unstable flow fields, researchers have drawn on the principle of Tuned Mass Dampers (TMD) from civil engineering.

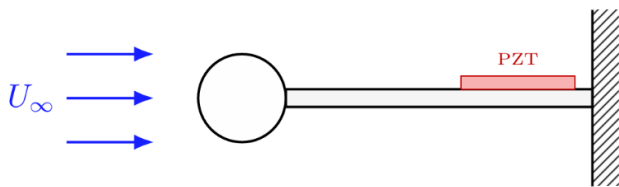


Figure 1. Single-degree-of-freedom direct harvesting system. Here, U_{∞} represents the free-stream velocity of the fluid, and PZT denotes the piezoelectric ceramic transducer used for energy conversion.

TMD, a milestone technology in vibration control, has demonstrated excellent reliability in multi-scale engineering scenarios since Frahm proposed the concept of dynamic vibration absorption in 1911 [21], and Den Hartog [22] further improved its parameter optimization theory. Its core logic lies in precisely tuning the natural frequency of the auxiliary mass block to be near the resonance frequency of the primary structure, achieving directional transfer of kinetic energy through the anti-phase motion between the two. In civil engineering, the wind-induced vibration TMD combination system deployed in the Taipei 101 Tower (Figure 2) is a landmark application of this technology [23]; in the aerospace field, TMD is also widely used to suppress wing flutter [24]. In modern energy harvesting research,

the role of TMD is shifting from a pure energy dissipator to an energy harvester. By replacing traditional damping elements with piezoelectric or electromagnetic transduction mechanisms, TMDs can utilize their amplification effect on the primary structure's vibration to significantly improve energy extraction efficiency in low-flow-speed environments.

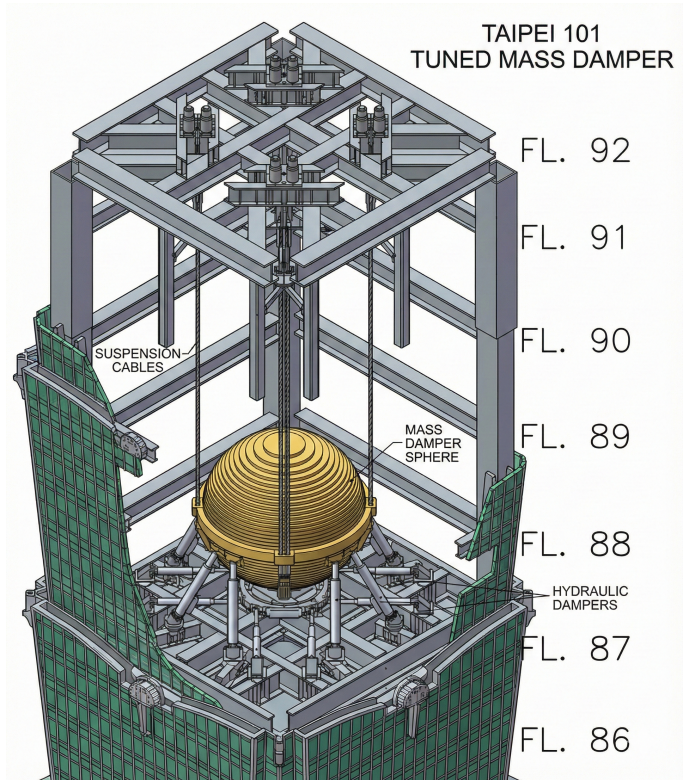


Figure 2. The pendulum of the main Tuned Mass Damper, a sphere made of stacked steel plates, swings within the upper stories of the tower.

Chao et al. [25] recently conducted in-depth research on linear TMD parameter optimization. Focusing on non-forced self-excited systems with TMD (Figure 3) and with NES (Figure 4), and utilizing Runge-Kutta numerical parameter scanning techniques based on systematic regression analysis of the optimal TMD response, they established high-precision empirical formulas for the optimal stiffness coefficient $\kappa_{T,fit}$ and optimal damping ratio β_{fit} for mass ratios m^* in the range of [0.01, 0.1]:

$$\kappa_{T,fit} \approx 1.051m^* - 0.007 \quad (2)$$

$$\beta_{fit} \approx 13459.19m^{*3} + 2479.74m^{*2} - 93.37m^* + 1.63 \quad (3)$$

These formulas provide benchmark parameters of significant scientific reference value for the initial design of TMDs for vibration suppression in practical engineering.

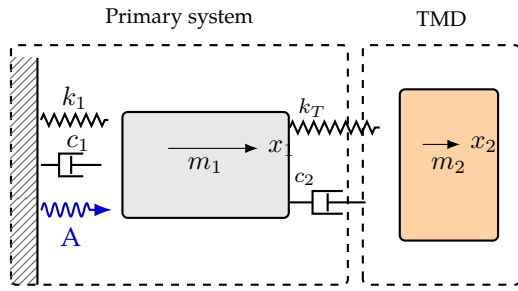


Figure 3. Nonlinear self-excited system coupled with a Tuned Mass Damper (TMD). Here, A indicates the external base excitation (Reproduced with permission from [28]).

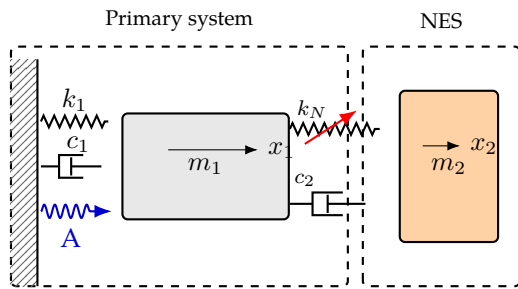


Figure 4. Nonlinear self-excited system coupled with a Nonlinear Energy Sink (NES) (Reproduced with permission from [28]).

Subsequent comparative studies showed that under forced vibration conditions, the optimized TMD exhibited comprehensive suppression performance and energy absorption potential superior to that of the Nonlinear Energy Sink (NES). Research indicates that when the excitation frequency $\Omega > 1.5$, the response suppression capability of the TMD is significantly better than that of the NES. The core physical mechanism for this difference lies in the activity level of the energy transmission channel. Since the restoring force of the NES has a cubic nonlinear relationship with its displacement (i.e., $f_{kn} = k_N(x_1 - x_2)^3$), under micro-amplitude vibrations generated by high-frequency excitation, its coupling force is extremely weak. This "Weak Coupling Effect" causes the energy transmission channel of the NES to be in a low-activity or even dormant state in the non-resonant region, making it difficult to achieve effective energy dissipation or capture.

In summary, under ideal frequency tuning and steady-state response conditions, the linear TMD demonstrates excellent vibration suppression capabilities and energy absorption potential. However, its practical application is limited by the high randomness and unsteadiness of the environmental flow field. The traditional linear design paradigm faces three core physical bottlenecks, which directly

constitute the endogenous driving force promoting the evolution of technology towards nonlinearity, lightweight design, and source enhancement (as shown in Figure 5) [26]:

- **Narrowband Bottleneck and Frequency Detuning Sensitivity:** The power gain of a linear system relies heavily on the resonant matching between the forcing frequency and the system's natural frequency. In a fluid environment, the excitation frequency f_s of vortex-induced vibration (VIV) follows the Strouhal relationship with the flow velocity U :

$$f_s = \frac{StU}{D} \quad (4)$$

where St is the Strouhal number and D is the characteristic length. The Equation (4) establishes a linear proportionality between f_s and U , any random fluctuation in flow velocity causes the excitation frequency to drift. Since the response bandwidth of a linear TMD is extremely narrow, once frequency detuning occurs, the system's energy transfer channel is instantly cut off. By introducing nonlinear stiffness, such as negative stiffness or bistable mechanisms, Targeted Energy Transfer (TET) can break the single resonance limit of linear systems [27, 28], achieving a broadband response and significantly enhancing the system's robustness to variable flow velocity environments [29, 30].

- **Physical Mass Dependency and Lightweight Constraints:** According to Den Hartog's classic optimization criteria [22], the efficacy of a linear absorber directly depends on the mass ratio (ratio of added mass to primary system mass). To obtain significant energy conversion efficiency, TMDs usually require a large additional physical mass, which is often strictly limited in structural design (typically capped at 0.1). This rigid demand for physical mass severely restricts the application of this technology in fields highly sensitive to payload, such as aerospace and Micro-Electro-Mechanical Systems (MEMS) [31]. Introducing inertial mass control (Path 2), such as the Tuned Mass Damper Inerter (TMDI), utilizes the "small mass, large inertia" characteristic of the Inerter to achieve mass decoupling, thereby maintaining extremely high energy absorption efficiency while reducing the system's physical self-weight [32].
- **Source Excitation Intensity Bottleneck:** In standard flow around a circular cylinder, the amplitude of VIV is usually self-limited by the fluid-structure interaction mechanism, with its

dimensionless amplitude A/D often hovering around 1.0 [33], physically limiting the stroke and work capacity of the harvester. Since the low-amplitude vibration of the primary structure limits the upper bound of energy input, backend optimization struggles to break through the physical maximum of flow field energy capture. Implementing flow field reconstruction and source enhancement, through means such as Passive Turbulence Control (PTC), surface roughness reconstruction, or Energy Concentration Pipes (ECP), artificially induces stronger nonlinear instabilities (such as galloping coupling), thereby actively capturing more kinetic energy from the flow field and increasing the overall power density.

Given the above limitations, the design of fluid energy harvesting systems is undergoing a profound paradigm shift from local linear optimization to multidimensional nonlinear synergy. As shown in Figure 5, future development trends no longer pursue breakthroughs in a single dimension in isolation but rather construct high-power-density systems capable of adaptive operation in complex flow fields through the deep integration of Nonlinear Stiffness + Inertial Amplification + Flow Field Control. How to transcend the bandwidth and mass constraints of linear theory and reveal the nonlinear energy flow mechanism under multi-physics coupling has become a key scientific proposition in the current field of fluid energy harvesting research.

5 Nonlinear Dynamics Regulation and Flow Control Strategies for FIV Energy Harvesting Systems

Addressing the frequency detuning and efficiency bottlenecks of classic linear TMD systems in complex marine flow fields, recent research in FIV energy harvesting has moved beyond single linear resonance toward multidimensional nonlinear synergy. As shown in Figure 6, the academic community is focusing on technological breakthroughs across three core dimensions: (1) breaking narrowband limits by introducing Nonlinear Energy Sink (NES) mechanisms; (2) achieving lightweight mass decoupling using Inerters; and (3) implementing source energy enhancement via Passive Turbulence Control (PTC). This chapter systematically reviews the evolutionary trajectory and enhancement mechanisms of these frontier configurations.

5.1 Frontier Configurations and Enhancement Mechanisms of NES

Given the startup threshold issues of traditional NES under low-frequency, micro-amplitude excitation, as well as the need for broadened bandwidth and adaptability, recent research has focused on deep structural innovation. This section explores four representative enhancement strategies: (1) synergistic mechanisms of linear and geometric nonlinear damping; (2) inverted pendulum structures introducing impact dynamics for transient high-energy pulses; (3) negative stiffness/bistable mechanisms to improve energy capture efficiency; and (4) time-varying stiffness to broaden the effective frequency band.

5.1.1 Novel NES Structure Combining Linear Damping and Geometric Nonlinear Damping

Addressing the limitations of traditional NES in energy capture and dissipation efficiency, Qi et al. [34] proposed a novel NES structure combining linear damping with geometric nonlinear damping (Figure 7). This study utilizes the geometric nonlinear effect produced by horizontally symmetrically arranged damping elements during vertical motion (Figure 8) to construct a nonlinear damping force in the form of $x^2\dot{x}$. Jing and Lang [35] found that cubic damping can effectively suppress peaks near the resonance frequency. Building on this, Al-Shudeifat et al. [36] employed a combination configuration where linear damping ensures basic energy dissipation capability during micro-tremors or initial stages, while nonlinear damping intervenes as amplitude increases, providing stronger dissipation stiffness and damping bandwidth.

Through the complex variable averaging method and slow invariant manifold analysis, the study revealed that this combined damping mechanism can effectively induce strongly modulated responses in the system, thereby significantly enhancing the efficiency of Targeted Energy Transfer (TET). Numerical simulation and analytical results show that compared to single damping forms (L-NES, G-NES), LG-NES demonstrates superior vibration suppression and energy harvesting efficiency under both pulse and harmonic excitations. This provides an important theoretical basis for designing nonlinear vibration energy harvesting systems that possess both wide bandwidth and high energy conversion efficiency.

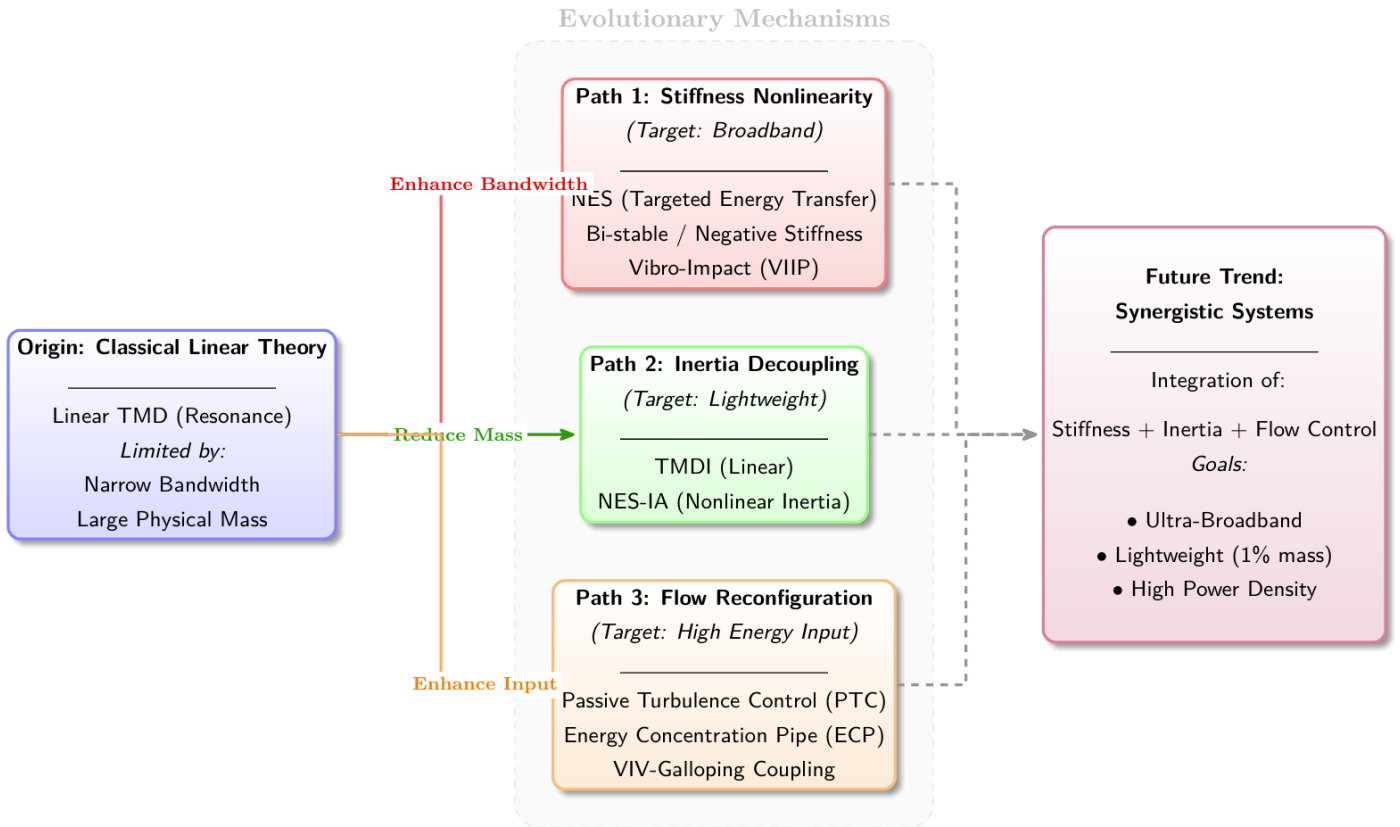


Figure 5. Evolutionary roadmap of flow-induced vibration energy harvesting systems.

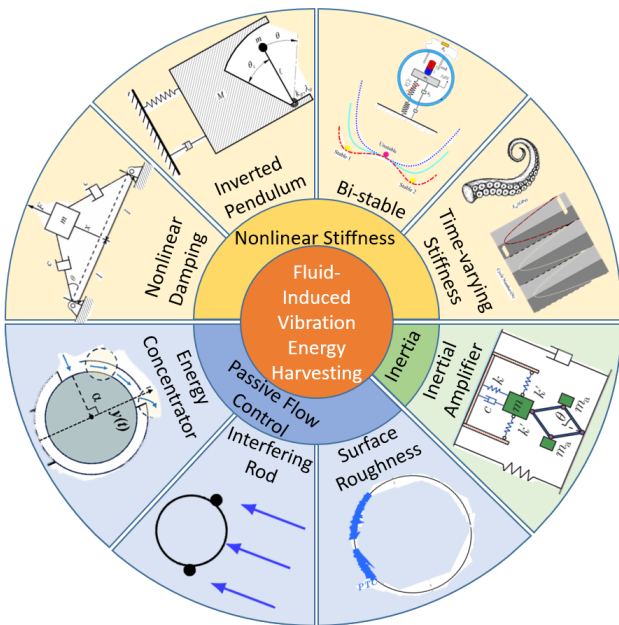


Figure 6. Current research status.

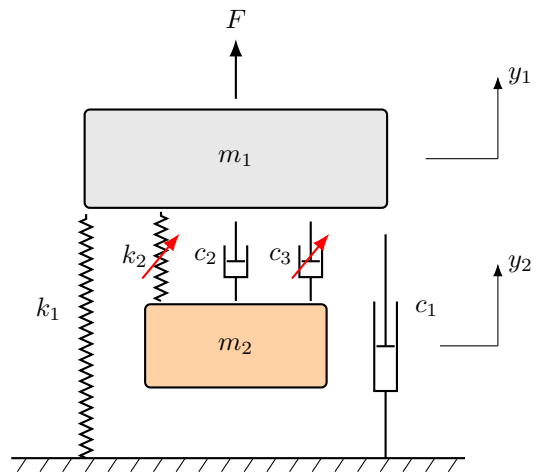


Figure 7. NES system model with linear damping and geometric nonlinear damping. Here, F denotes the external force (Reproduced with permission from [34]).

5.1.2 Inverted Pendulum Vibro-Impact NES

Targeting the efficient capture of impulsive vibration energy, Saeed et al. [37, 38] proposed a rotary NES that utilizes inertial coupling to convert the translational energy of the primary system into the rotation of a mass block, achieving rapid energy dissipation within

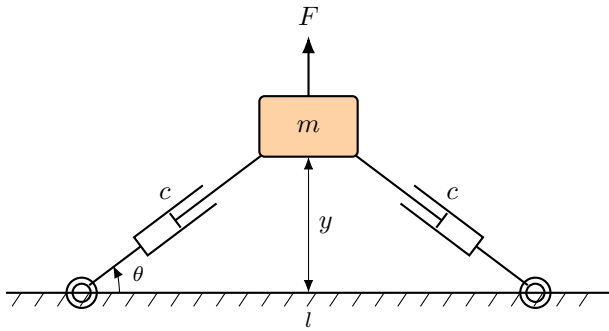


Figure 8. Schematic of geometric nonlinear damping (Reproduced with permission from [34]).

three oscillation cycles. Subsequently, Gendelman and Alloni [39] proposed a novel Vibro-Impact Inverted Pendulum NES (VIIP NES) (Figure 9), integrating bistability, rotational inertial coupling, and non-smooth vibro-impact characteristics [40].

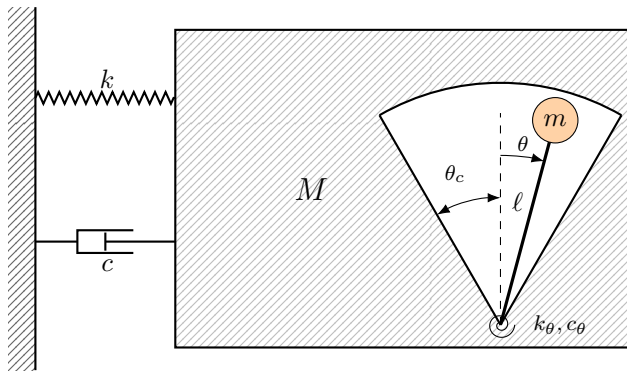


Figure 9. Schematic of a linear oscillator coupled with a Vibro-Impact Inverted Pendulum (VIIP) NES. k_θ and c_θ are the torsional stiffness and damping; θ is the rotational angle, and θ_c denotes the critical impact angle (Reproduced with permission from [40]).

First, the device utilizes the bistable characteristic of the inverted pendulum (gravity moment greater than restoring moment). A minute initial external vibration triggers the pendulum to overcome the instability of the equilibrium point and accelerate to one side (negative linear stiffness), solving the high startup threshold problem of traditional harvesters. Second, through the rotational inertial coupling mechanism, the translational energy of the primary system is rapidly converted into the rotational kinetic energy of the pendulum, accumulating significant velocity before contacting the wall. Finally, when the pendulum rotates to a preset angle, the accumulated kinetic energy is released instantly through non-smooth rigid collision, completing the transfer and capture of the vast majority of energy within the first half-cycle of oscillation.

Numerical analysis indicates that at the moment of the first impact, the velocity of the primary system drops by up to 96%, implying that most mechanical energy is instantly extracted. Although this study aimed at rapid vibration reduction, the verified half-cycle rapid energy transfer mechanism provides a valuable reference for designing high-power-density pulse energy harvesters. By replacing the rigid wall collision energy dissipation in the paper with piezoelectric impact transduction or electromagnetic induction transduction, this structure is particularly suitable for Impulsive or Shock environmental vibration energy harvesting (e.g., pulse flow) [41].

5.1.3 Bistable Configuration Integrated with Adjustable Negative Stiffness

Addressing the wide frequency band and strong nonlinearity of FIV energy distribution, Huang and Zhong [42] proposed an Electromagnetic Bi-stable Energy Harvester (EBEH) integrated with adjustable negative stiffness. The study established a dynamic model coupling a Wake Oscillator and a Structural Oscillator, introducing negative linear stiffness to reshape the system's potential energy function and constructing a nonlinear restoring force with double potential well characteristics.

The system consists of a primary structure (hollow cylinder) placed in the flow field and an internal EBEH (Figure 10). To describe the dynamic behavior, a comprehensive mathematical model including a fluid mechanics model, structural dynamics model, and electromechanical coupling equations was established.

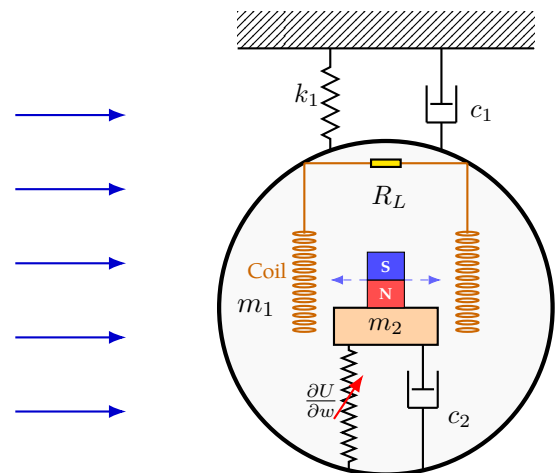


Figure 10. Schematic of the 2-DOF flow-induced vibration energy harvester. Here, R_L is the external load resistance, and $\partial U / \partial w$ represents the bistable nonlinear restoring force (Reproduced with permission from [42]).

(1) Wake Oscillator and Nonlinear Fluid Model

To effectively simulate the fluid's effect on the structure in a reduced-order model, the Van der Pol equation [43] is introduced to describe the dynamic variation of the lift coefficient. The fluid dynamic force (Vortex-Induced Force, F_{VIV}) acting on the cylinder is composed of a lift term related to vortex shedding and a fluid damping term:

$$F_{VIV} = \frac{1}{2}C_{L0}\rho DU_0^2 L \cdot r - \frac{1}{2}C_D\rho DU_0 L \cdot \dot{y}_1 \quad (5)$$

where r is the dimensionless wake variable representing lift coefficient fluctuation. Its dynamics are governed by the modified Van der Pol equation:

$$\dot{r} + \Lambda\omega_s(r^2 - 1)r + \omega_s^2 r = \frac{A}{D}\ddot{y}_1 \quad (6)$$

(2) Structural Dynamics Equations

The system is modeled as a two-degree-of-freedom (2-DOF) coupled oscillation system. Equation of motion for the Primary System (Cylinder m_1):

$$m_1\ddot{y}_1 + c_1\dot{y}_1 + k_1y_1 - (c_2 + c_e)\dot{w} - \frac{\partial U}{\partial w} = F_{VIV} + F(t) \quad (7)$$

Equation of motion for the Internal Harvester (Mass m_2): Let $w = y_2 - y_1$ be the relative displacement.

$$m_2(\ddot{w} + \ddot{y}_1) + (c_2 + c_e)\dot{w} + \frac{\partial U}{\partial w} = 0 \quad (8)$$

(3) Bistable Nonlinear Restoring Force and Potential Function

The core innovation lies in introducing nonlinear stiffness to construct bistable characteristics. The potential energy derivative (restoring force) is defined as:

$$\frac{\partial U}{\partial w} = k_3w + k_2w^3 \quad (9)$$

Specifically, the model sets $k_3 < 0$, making the system bistable. This introduction of nonlinear stiffness alters the system's dynamic topology, enabling large-amplitude inter-well snap-through at specific excitation levels, thereby significantly increasing amplitude and energy capture efficiency.

(4) Electromechanical Coupling and Power Output

Assuming the induced electromotive force is proportional to the relative velocity, the electromagnetic damping force F_{em} is:

$$F_{em} = k_e \cdot \dot{Q} \approx c_e \cdot \dot{w} \quad (10)$$

The instantaneous output power $P(t)$ depends on the load resistance R_L :

$$P(t) = R_L \dot{Q}^2 = c_e \dot{w}^2 \quad (11)$$

Research indicates that the bistable mechanism is key to improving energy capture efficiency. Numerical simulations and CFD validation show that the bistable system can induce large-amplitude snap-through motion [44], greatly enhancing TET efficiency. Data shows that in the 20–30 m/s flow velocity range, the EBEH's nonlinear energy transfer efficiency exceeds 60%, and its maximum average output power is increased by over 900% compared to traditional cubic stiffness harvesters. It should be noted that such substantial performance gains are highly condition-specific; this 900% relative increment is heavily dependent on the specific structural mass ratio ($\mu = 0.05$) and the transition from a mono-stable (cubic) to a bi-stable configuration under specific high-velocity aerodynamic excitations. Therefore, these quantitative enhancements reflect the superiority of the bi-stable mechanism within its specific theoretical framework rather than an absolute, universally applicable power scaling factor. This strongly proves the significant advantages of bistable nonlinearity in broadening FIV energy harvesting bandwidth and improving power density [45].

Furthermore, the article reveals the design trade-off law of "Negative Stiffness Regulation and Flow Velocity Matching":

- **Startup Threshold vs. High-Energy Orbit:** Smaller negative stiffness corresponds to a lower potential barrier, facilitating the activation of nonlinear jumps at low flow velocities for early startup; however, larger negative stiffness, while raising the startup threshold, can maintain a deeper high-energy orbit in the high flow velocity range, thereby achieving stronger TET capability.
- **Synergistic Effect of Hybrid Excitation:** Under low flow velocity conditions where the vortex-induced force alone is insufficient to overcome the potential barrier, introducing base excitation (e.g., bridge vibration) acts as a catalyst [46], assisting the oscillator in crossing the barrier into an efficient inter-well motion state. This confirms the device's excellent robustness in complex multi-source excitation environments.

5.1.4 Synergy of Bio-inspired Time-varying Stiffness and Surface Roughness

Addressing the limited bandwidth and low efficiency of FIV energy harvesters in complex flow fields, Wu et al. [47], inspired by the biomechanics of octopus tentacles [48], proposed a synergistic enhancement mechanism combining Time-varying Stiffness and Passive Turbulence Control (PTC) [49] (Variable Stiffness Coupled with PTC System, VSPTCS).

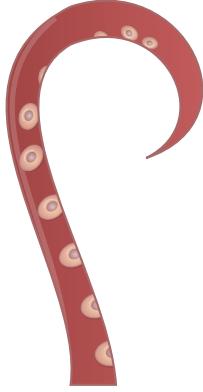


Figure 11. Octopus tentacle model with variable stiffness.

Mimicking the variable stiffness of octopus muscles and the boundary layer control of suckers, the study arranges roughness strips (PTC) on the cylinder surface to manage the local instability caused by dynamic stiffness changes, thereby maximizing energy capture while maintaining global system stability (Figure 11). Numerical simulations show that this coupling of rigidity and flexibility mechanism significantly alters the wake structure. By inducing high-energy VIV, the energy harvesting efficiency reaches a maximum of 57% (approximately twice that of a traditional bare cylinder), and the vibration amplitude is increased by 11 times. However, it is important to clarify that this 11-fold amplitude surge and 57% peak efficiency are achieved under precisely tuned time-varying stiffness modulation and specific PTC coverage parameters within a designated low Reynolds number subcritical flow regime ($1.2 \times 10^4 - 2.4 \times 10^4$). These values demonstrate the potential of active-passive coupling but are not universally scalable across all flow conditions.

The time-varying stiffness (Figure 12) is defined as:

$$K_{vt} = \frac{K_0}{2} \times \sin(m \times \omega_n \times t) + K_{off} \quad (12)$$

where $K_{vt}(t)$ denotes the imposed time-varying stiffness, modeled as a sinusoidal modulation around

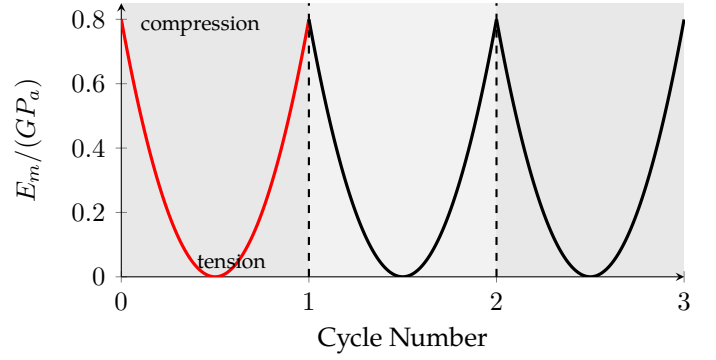


Figure 12. variable Stiffness over time.

an offset K_{off} . K_0 is the modulation amplitude, and t is time. The modulation frequency is set to $\omega_v = m \omega_n$, where ω_n is the natural frequency of the baseline (constant-stiffness) system in still water and m is a dimensionless frequency ratio controlling the stiffness-variation rate. The offset K_{off} is chosen to keep $K_{vt}(t)$ positive and within a prescribed physical range.

This research not only proves the feasibility of using time-varying stiffness to broaden the frequency band at low Reynolds numbers ($1.2 \times 10^4 - 2.4 \times 10^4$) but also reveals the critical role of passive flow control in stabilizing the instability of nonlinear systems.

5.2 Novel NES Structure Combined with Inertial Amplifier

The concept of the Inerter was first proposed by Professor Malcolm Smith at the University of Cambridge in 2002 [50]. It is a two-terminal mechanical element where the force produced is proportional to the relative acceleration between the terminals. The ideal mechanical model of an inerter can be expressed by the following equation:

$$F = b(\dot{v}_2 - \dot{v}_1) \quad (13)$$

where F is the force generated, v_1 and v_2 are the velocities of the two terminals, $(\dot{v}_2 - \dot{v}_1)$ is the relative acceleration, and b is the inertance (unit: kg).

Addressing the limitation that traditional NES requires a large additional mass (typically 5%–10% of the primary system mass) for low-frequency energy absorption, Zhang et al. [51] proposed a novel NES combined with an Inertial Amplifier (NES-IA) (Figure 13). This structure utilizes the geometric nonlinear characteristics of a linkage mechanism to adjust the inertance angle, converting a small physical mass into a massive equivalent dynamic mass (inertial amplification), thereby achieving the

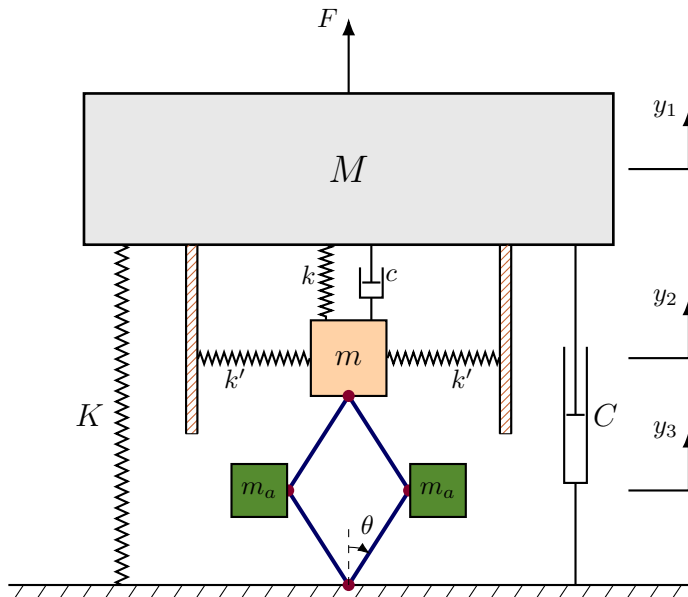


Figure 13. Primary oscillator coupled with an NES and Inertial Amplifier (NES-IA). m_a represents the mass of the inertial amplifier (Reproduced with permission from [51]).

effect of "small mass, large inertia". Furthermore, the study resolved the issue of asymmetric nonlinear stiffness caused by gravity in the vertical direction through a special spring pre-compression/pre-tension configuration (stretching spring k to offset gravity while compressing k' to offset the first-order elastic coefficient), constructing a pure cubic nonlinear stiffness [52].

Numerical and analytical results indicate that the system can achieve a vibration reduction efficiency of up to 85.11% under harmonic excitation with only 1% actual added mass. Under shock excitation, it effectively triggers High-Frequency Resonance Capture (HFRC). It is worth emphasizing that this 85.11% suppression efficiency is analytically validated under targeted harmonic excitation frequencies where the inertial amplification effect is fully activated. Translating this apparent mass efficiency to field deployments with random, broadband turbulence may yield different operational efficiencies. Although the original study aimed to maximize energy dissipation for vibration reduction, its core mechanism—efficient Targeted Energy Transfer (TET)—aligns highly with energy harvesting demands. By replacing the viscous damping in the original system with an electromechanical transduction damper with controllable load, and re-optimizing the damping matching coefficient to maximize power output rather than minimizing structural displacement, this structure holds promise for conversion into a

high-density energy harvesting device.

5.3 Energy Capture Enhancement Based on Passive Flow Control and Morphological Reconstruction

The exploration of hydrodynamic energy harvester performance has evolved from utilizing single vibration modes to coupled multi-mode control. Early research focused on Vortex-Induced Vibration (VIV) [53, 54], but despite its low startup flow velocity, it suffers from narrow bandwidth and low efficiency at high flow velocities. To overcome these limitations, researchers began introducing the Galloping mechanism [55], an unstable response capable of continuously increasing amplitude with flow velocity, thereby significantly enhancing power output at high speeds.

Passive Turbulence Control (PTC) technology provides an effective path for coupling these two vibration modes. Early research, such as that by the Marine Renewable Energy Laboratory (MRELab) at the University of Michigan, proposed inducing galloping by arranging local roughness on the cylinder surface [56]. Subsequently, the research focus shifted to the impact of physical attachments (e.g., rods, strips, fins).

This section explores source governance strategies that alter the external morphology of the primary structure or the physical environment of the flow field. By introducing interference rods, internal jets, and square prism coupling, these passive control means directly intervene in the wake vortex shedding mode, thereby enhancing fluid energy input to the structure at the source and achieving a leap in energy harvesting efficiency.

5.3.1 Wide Flow Range Mode Switching Using Interference Rods (SSR)

Addressing the narrow bandwidth and low efficiency of cylindrical VIV energy harvesters at high flow velocities, experimental studies by Hu et al. [57] and Park et al. [58] confirmed that the installation position of PTC attachments has a far more significant impact on FIV than their geometric shape. Early optimization studies focused on the front region of the cylinder; for instance, Ding et al. [59] found that installing fin-shaped rods at 60° yielded higher output power.

Building on this, Sun et al. [60] proposed an enhancement strategy using PTC. By symmetrically installing Square-Shaped Rods (SSR) on the cylinder surface and adjusting their installation angle, the

study successfully induced VIV-Galloping coupling. Experiments showed that when the interference rods were installed at 150° , the system could start with VIV in the low flow velocity region and seamlessly switch to the large-amplitude galloping mode in the high flow velocity region, achieving the highest mechanical power output over a wide flow range.

The article defines total energy efficiency and energy extraction efficiency as follows:

$$P_w = \frac{1}{2}\rho U^3(2A_y + D)L \quad (14)$$

Note: The use of $(2A_y + D)$ as the swept area is higher than the standard calculation but more realistically reflects the range of interaction between the system and the fluid.

$$\eta_{He} = \frac{P_{Mech}}{P_w \times \text{Betz Limit}} \quad (15)$$

where P_{Mech} is the energy pushing the cylinder's vibration, obtained by integrating the fluid force F_y multiplied by the cylinder velocity \dot{y} and Betz Limit equals $16/27$ [61].



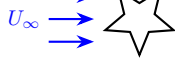
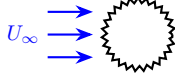
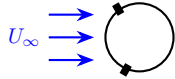
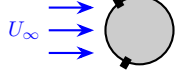
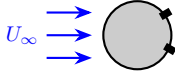
Based on the TOPSIS (Technique for Order of Preference by Similarity to Ideal Solution) method, a horizontal comparison with other structural designs (Table 1) confirmed that the 150° back-flow design exhibits the most intense oscillation, effectively overcoming amplitude decay outside the VIV resonance zone.

5.3.2 Energy Concentration Pipe (ECP): Passive Wake Control Based on Internal Jet Mechanism

Jet control has long been used to suppress vibrations in bridges or cables. Chen et al. [67] utilized perforated shells to achieve passive jets (suction on the windward side, blowing on the leeward side), successfully reducing drag by 33.7% and fluctuating wind load by 90.6%. Wang et al. [68] hypothesized that since jets can cancel vortex strength, changing the jet angle and configuration could conversely strengthen vortices. Traditional cylinders allow part of the airflow to dissipate from the sides. The Energy Concentration Pipe (ECP) directs this otherwise wasted energy through an internal channel to the wake core region, a phenomenon defined as the Energy Concentration Phenomenon.

To break the startup bottleneck and narrow bandwidth of FIV harvesters at low flow velocities, Wang et al. [69] proposed a passive flow control strategy based on

Table 1. Cross-section configurations and EWM-TOPSIS scores from previous studies.

Cross Section	Configuration	Score
Square [62]		0
Tandem diamond cylinders [62]		0.368
Star-shaped cylinder [63]		-
Cylinder with roughness [64]		0.465
Cylinder with large PTC ($\theta = 60^\circ, H/D = 0.15$) [65]		0.576
Cylinder with large PTC ($\theta = 60^\circ, H/D = 0.10$) [66]		0.733
SSR-cylinder ($\theta = 150^\circ$) [60]		0.754

ECP. The device innovatively designs a flow channel inside the cylinder (Figure 14), utilizing the dynamic pressure on the windward side to suck in airflow and eject it at high speed from the sides, forming a passive jet directly injected into the wake zone [69].

Experiments and numerical simulations show that this mechanism significantly alters the wake vortex shedding mode [70], inducing intense transverse oscillation of wake vortices. Specifically, with a symmetric double-outlet ($60^\circ, 60^\circ$) configuration, the effective Lock-in Region of the harvester was broadened by 108.33% compared to the baseline cylinder, and the maximum output voltage increased by 12.69%. As is common when evaluating FIV attachments, this 108% lock-in expansion is specific to the moderate Reynolds number regime tested and is measured relative to a standard bare cylinder. Direct comparisons of such percentages across different studies must account for variations in mechanical damping, structural aspect ratios, and baseline definitions. This proves that precision guiding fluid kinetic energy to the wake core via passive jets is a highly efficient pathway for source enhancement.

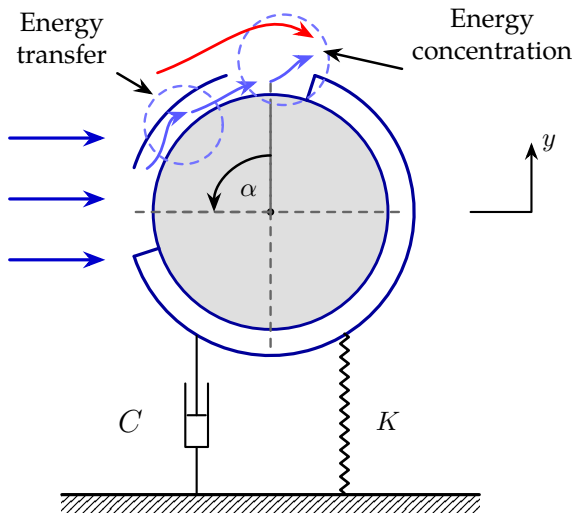


Figure 14. Schematic of Energy Concentration FIVPEH VIV of bluff body (Reproduced with permission from [68]).

5.3.3 Weak and Strong Coupling Mechanisms of VIV and Galloping

Huang et al. [71] systematically studied the response characteristics of NES in different hydrodynamic environments based on a Structure-Wake Oscillator coupled model. Using a Van der Pol oscillator to simulate the unsteady characteristics of the wake, the study investigated two vibrating structures: a circular cylinder (Figure 15) (pure VIV) and a square prism (VIV + Galloping) [72] (Figure 16).

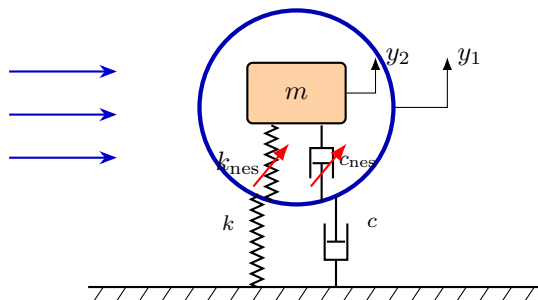


Figure 15. Vibrating cylinder prism installed with NES (Reproduced with permission from [71]).

The results reveal the decisive influence of fluid-structure coupling strength on NES energy transfer efficiency. In cylindrical VIV and weak-coupling square prism systems (where VIV and galloping flow velocity domains are separated), the NES demonstrates excellent energy absorption. Particularly in the galloping phase of the weak-coupling square prism, the NES can attenuate the primary structure's amplitude by up to 70% via Targeted Energy Transfer (TET). The introduction of NES compared to the uncontrolled state significantly suppresses the amplitude in the VIV stage and delays

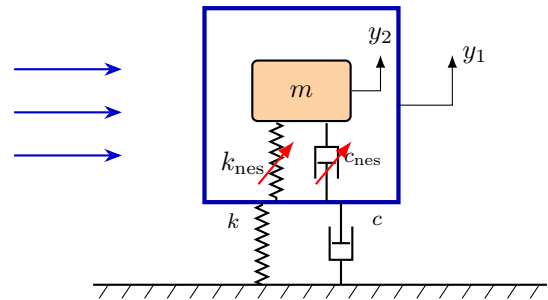


Figure 16. Vibrating square prism installed with NES. (Reproduced with permission from [71]).

the onset of galloping. From an energy harvesting perspective, this implies that the vast majority of energy input by the fluid is successfully transferred to the NES subsystem via nonlinear stiffness, predicting a very high potential output power density in such conditions.

However, under strong coupling galloping conditions, where VIV and galloping interact strongly, the efficacy of the NES is significantly limited. The study found that the NES struggles to maintain an effective energy transfer channel, and its suppression effect drops drastically. This offers a crucial avoidance strategy for harvester design: in flow fields dominated by strong aerodynamic instability, a simple NES structure may fail to effectively extract energy.

6 Conclusion

Flow-Induced Vibration (FIV) energy harvesting exploits flow-induced instabilities—such as Vortex-Induced Vibration (VIV), galloping, flutter, and wake/array interference—to convert environmental fluid kinetic energy into structural vibration, which is subsequently transduced into electrical energy via piezoelectric, electromagnetic, or triboelectric mechanisms. Over the past two decades, a systematic research landscape has emerged, evolving from single-degree-of-freedom direct harvesting to absorber-based/multi-degree-of-freedom configurations, with increasing emphasis on comprehensive indicators such as wide flow velocity range, broad bandwidth, robustness, and engineering feasibility. High-level reviews indicate that the core challenge of FIV energy harvesting is not merely whether resonance occurs, but how to achieve sustainable, high-stability energy input and controllable energy concentration paths under backgrounds of flow velocity fluctuations, turbulence disturbances, parameter drift, and strong fluid-structure interaction nonlinearity [54].

Table 2. Summary and critical comparison of contemporary absorber-based FIV energy harvesting mechanisms.

Configuration	Flow Conditions	Evidence	Advantages	Limitations
Classic TMD	Narrowband	Analyt. / Num.	Straightforward to implement; provides good suppression in narrow frequency range.	Sensitive to frequency detuning; requires larger physical added mass.
LG-NES	Harmonic / Impulsive excitations	Analyt. / Num.	Broader effective frequency band; strong modulation response (SMR) helps dissipate energy quickly.	Complex mechanical implementation (symmetrical horizontal dampers).
VIIP NES	Impulsive	Analyt. / Num.	Achieves complete vibration suppression during the first half-cycle of oscillation.	Non-smooth inelastic collisions may cause structural fatigue; complex setup.
EBEH	VIV to Galloping	Analyt. / Num. (CFD)	High nonlinear transfer efficiency (>60%); >900% power increase over monostable.	Needs sufficient flow or base excitation to cross barrier for inter-well snap-through.
NES-IA	Harmonic and impulsive excitations	Analyt. / Num.	Attenuates steady-state and transient responses with ultralow physical mass (e.g., 1%).	Unreasonable parameter designs may trigger higher branch/high-frequency resonance.
VSPTCS	$(1.2 \times 10^4 - 2.4 \times 10^4) Re$	Exp. / Num. (CFD)	Up to 11× amplitude surge & doubles harvesting efficiency up to 57%.	Time-varying stiffness requires active energy input to modulate.
PTC-SSR	VIV to Galloping	Exp.	Excites VIV-galloping coupling to avoid high-speed amplitude decay.	Extremely sensitive to installation angle (some angles suppress vibration).
ECP	VIV	Exp. / Num. (CFD)	Symmetrical dual outlet expands lock-in region by 108.33% and boosts voltage.	Asymmetrical or improperly angled single outlets (e.g., 90°) can suppress vibration.

Classic linear tuning concepts (e.g., TMD) provide clear physical images and analytical design criteria for absorber-based harvesters. However, they inherently rely on narrowband tuning. In FIV, the excitation frequency typically varies with flow velocity and is accompanied by lock-in regions, added mass effects, and wake unsteadiness, making detuning—efficiency collapse almost inevitable. Furthermore, the effectiveness of linear absorbers is often strongly correlated with the mass ratio, creating a hard constraint between miniaturization/lightweighting

and high output. In contrast, more promising routes in recent years involve reducing dependence on precise tuning through nonlinear mechanisms and inertial amplification, or enhancing source-end harvestable energy and locking stability through flow field reconstruction, thereby improving the device's stable output capability across a wide range of operating conditions.

Synthesizing existing research progress, the FIV-EH field exhibits three clear evolutionary threads: (i)

Broadbandization dominated by stiffness nonlinearity (NES/multi-stable/impact energy sinks); (ii) Lightweighting based on inertial amplification/mass decoupling (Inerter); and (iii) Flow regulation oriented towards source-end gain (passive/semi-active wake reconstruction, energy concentration channels). These three paths respond to the most critical engineering pain points—low startup, wide operating conditions, and deployability—from the dimensions of structural bandwidth extension, equivalent mass enhancement, and flow field energy input enhancement, respectively. These three paths and their corresponding enhancement mechanisms are comprehensively summarized and critically compared in Table 2.

7 Future Perspectives

This paper reviews the evolution of FIV energy harvesting systems from linear resonance to multidimensional nonlinear synergy. Existing research indicates that single linear designs can no longer meet the demands for broadband, lightweight, and high-efficiency performance. Future technological breakthroughs will focus on the following six disciplinary dimensions:

7.1 Fluid Mechanics: Cylinder Arrays and Wake Synergy

Future research will shift from optimizing single oscillators to the synergistic enhancement of Cylinder Arrays. By rationally designing the spacing ratio (S/D) and geometric configuration of oscillators, and utilizing the positive interference of upstream wakes on downstream oscillators (Wake-induced Galloping), the secondary distribution and maximized capture of flow field energy in space can be realized.

7.2 Bionics: Evolutionary Wisdom and Morphological Adaptation

Deeply drawing from the evolutionary wisdom of marine organisms allows for leapfrog breakthroughs in dynamic efficiency. Key focuses include introducing bio-inspired structures, such as D-shaped Bionic Fins [73], to simulate the high-frequency oscillatory propulsion modes of fish to reduce drag; or combining the time-varying stiffness of octopus tentacles to endow systems with complex environmental adaptability, significantly improving overall execution efficiency.

7.3 Nonlinear Dynamics and Control Theory

- **Multi-directional Vibration Adaptation and Stochastic Resonance:** Addressing the variable flow direction in real flow fields, developing Multi-directional NES has become a frontier. Orthogonal coupled structures can realize self-tuned responses under arbitrary excitation directions. Furthermore, combining Stochastic Resonance theory can transform environmental turbulence noise into useful auxiliary excitation, enhancing stability under complex flow fields.
- **Reliability-Based Design Optimization (RBDO):** Nonlinear systems are highly sensitive to parameter perturbations; purely pursuing peak power often leads to high experimental efficiency but poor practicality. Future research must introduce reliability optimization theory, shifting from seeking the optimal solution under a single condition to the most robust solution over the full life cycle, balancing energy capture efficiency with system failure risk.

7.4 Computer Science and Artificial Intelligence

Physics-Informed Deep Learning and Topology Optimization: Utilizing Neural Differentiable Models or deep learning to replace expensive CFD simulations enables real-time mapping and rapid topology optimization for high-dimensional Fluid-Structure Interaction (FSI) problems. Introducing Digital Twin technology allows for full life-cycle performance mapping of equipment. Through self-sensing and adaptive algorithms, real-time intelligent tuning of system parameters with flow velocity fluctuations can be achieved, solving the poor performance of passive systems under extreme variable conditions [74].

7.5 Materials Science: Hybridization and Durability

- **Hybrid Energy Conversion:** Integrating Piezoelectric (PEH), Electromagnetic (EMG), and Triboelectric Nanogenerators (TENG) to construct hybrid systems exploits the high voltage advantage of TENG at low frequencies and the high power characteristics of electromagnetic systems at high frequencies, achieving full-spectrum coverage.
- **Extreme Environment Tolerance and Anti-Biofouling:** Developing bio-inspired anti-fouling coatings with self-healing capabilities or self-cleaning systems is crucial to solve structural morphology changes and efficiency decay caused

by Biofouling in deep-sea environments, ensuring long-term structural consistency.

7.6 Power Electronics and System Integration

Addressing the fluctuating signals generated by nonlinear vibrations, developing low-power adaptive Maximum Power Point Tracking (MPPT) circuits and nonlinear interface circuits (such as Synchronized Switch Harvesting on Inductor, SSHI) is essential to overcome bottlenecks in backend storage and rectification efficiency.

7.7 Bridging the Numerical-Experimental-Field Validation Gap

To translate current laboratory successes into commercial viability, future research must prioritize bridging the substantial gap between numerical simplifications, idealized experiments, and real-world marine deployments.

Transitioning from 2D Sweeps to High-Fidelity 3D Modeling

While current research heavily relies on two-dimensional (2D) computational fluid dynamics (CFD) for initial parameter sweeps, future numerical paradigms must transition towards high-fidelity three-dimensional (3D) modeling. As the operating environment shifts to subcritical or supercritical flow regimes ($Re > 10^4$), 3D wake instabilities—such as vortex stretching and spanwise correlation loss—become highly pronounced. 2D simulations artificially enforce spanwise coherence, inevitably leading to a significant overestimation of fluctuating lift coefficients and structural amplitudes [75]. Therefore, for future harvesters with large aspect ratios or complex geometric attachments (e.g., ECP or PTCs), employing 3D simulations (such as Large Eddy Simulation, LES, or Detached Eddy Simulation, DES) will be mandatory to accurately capture critical flow features like tip vortices and spanwise separation [76].

Overcoming the Idealized Laboratory Constraints

Furthermore, a critical future challenge lies in overcoming the limitations of current experimental validations. Most testing is conducted in highly controlled water channels with uniform flow, minimal structural damping (c), and precisely tuned mass ratios (m^*). However, field deployment introduces profound physical uncertainties that future designs must anticipate:

1. Mass Ratio Variability and Biofouling: In practical marine environments, the inevitable occurrence of biofouling (e.g., attachment of

barnacles) dynamically alters the structure's surface roughness and effective mass. This uncontrolled mass addition can severely shift the natural frequency of the harvester, neutralizing the carefully tuned lock-in region [54]. Future materials and structures must inherently account for or resist this mass drift.

2. Parasitic Damping in PTO Systems: Unlike the idealized, low-friction constraints used in laboratories (e.g., air bearings), actual deployments require robust mechanical sealing for Power Take-Off (PTO) systems to prevent water ingress. Such sealing, combined with prolonged mechanical wear, introduces highly nonlinear and time-varying parasitic damping [20]. Ultimately, the next generation of FIV energy harvesting research must shift from deterministic optimization under ideal conditions to stochastic modeling and robust parameter design, ensuring systems can tolerate the inherent uncertainties of mass and damping in actual ocean deployments.

Data Availability Statement

Not applicable.

Funding

This work was supported by the National Natural Science Foundation of China under Grant U2341231 and Grant 52575091.

Conflicts of Interest

The authors declare no conflicts of interest.

AI Use Statement

The authors declare that no generative AI was used in the preparation of this manuscript.

Ethical Approval and Consent to Participate

Not applicable.

References

- [1] IEA (2025). World Energy Outlook 2025. IEA, Paris. Retrieved from <https://www.iea.org/reports/world-energy-outlook-2025>
- [2] NDRC (National Development and Reform Commission). (2021, October 24). Working guidance for carbon dioxide peaking and carbon neutrality

- in full and faithful implementation of the new development philosophy. Retrieved from https://en.ndrc.gov.cn/policies/202110/t20211024_1300725.html
- [3] CPC Central Committee. (2025, October 28). *Recommendations of the CPC Central Committee for formulating the 15th five-year plan for national economic and social development*. IDCPC. Retrieved from https://www.idcpc.org.cn/english2023/ttxw_5749/202510/t20251029_167976.html
- [4] Chengliang, H. (2026). Pursuing Green Development: From the 14th to the 15th Five-Year Plan. *China Economist*, 21(2), 89-119.
- [5] Wang, Y., Qin, J., & Lin, L. (2026, February). Discussion on Energy Economy and Optimization of Energy Structure. In *2025 7th Management Science Informatization and Economic Innovation Development Conference (MSIEID 2025)* (pp. 229-241). Atlantis Press. [CrossRef]
- [6] Mork, G., Barstow, S., Kabuth, A., & Pontes, M. T. (2010, January). Assessing the global wave energy potential. In *International conference on offshore mechanics and arctic engineering* (Vol. 49118, pp. 447-454). [CrossRef]
- [7] Khan, M. Z. A., Khan, H. A., & Aziz, M. (2022). Harvesting energy from ocean: Technologies and perspectives. *Energies*, 15(9), 3456. [CrossRef]
- [8] Qiu, T., Zhao, Z., Zhang, T., Chen, C., & Chen, C. P. (2019). Underwater Internet of Things in smart ocean: System architecture and open issues. *IEEE transactions on industrial informatics*, 16(7), 4297-4307. [CrossRef]
- [9] Liu, L., Guo, X., Liu, W., & Lee, C. (2021). Recent progress in the energy harvesting technology—from self-powered sensors to self-sustained IoT, and new applications. *Nanomaterials*, 11(11), 2975. [CrossRef]
- [10] Nordfjord, S. J., Thorsteinsson, S. E., & Andersen, K. (2025). Powering underwater robotics sensor networks through ocean energy harvesting and wireless power transfer methods: Systematic review. *Journal of Marine Science and Engineering*, 13(9), 1728. [CrossRef]
- [11] McPhaden, M. J., Connell, K. J., Foltz, G. R., Perez, R. C., & Grissom, K. (2023). Tropical ocean observations for weather and climate. *Oceanography*, 36(2/3), 32-43.
- [12] Shinohara, M., Araki, E., Mochizuki, M., Kanazawa, T., & Suyehiro, K. (2009). Practical application of a sea-water battery in deep-sea basin and its performance. *Journal of Power Sources*, 187(1), 253-260. [CrossRef]
- [13] Naqvi, A., Ali, A., Altabay, W. A., & Kouritem, S. A. (2022). Energy harvesting from fluid flow using piezoelectric materials: a review. *Energies*, 15(19), 7424. [CrossRef]
- [14] Abdelkareem, M. A., Ayoub, M., Khuri, S., Alami, A. H., Sayed, E. T., Deepa, T. D., & Olabi, A. G. (2023). Environmental aspects of batteries. *Sustainable Horizons*, 8, 100074. [CrossRef]
- [15] Han, J. Y., & Jung, S. (2022). Thermal stability and the effect of water on hydrogen fluoride generation in lithium-ion battery electrolytes containing LiPF₆. *Batteries*, 8(7), 61. [CrossRef]
- [16] Guillou, N., Lavidas, G., & Chapalain, G. (2020). Wave energy resource assessment for exploitation—a review. *Journal of Marine Science and Engineering*, 8(9), 705. [CrossRef]
- [17] Alford, M. H., Peacock, T., MacKinnon, J. A., Nash, J. D., Buijsman, M. C., Centurioni, L. R., ... & Tang, T. Y. (2015). The formation and fate of internal waves in the South China Sea. *Nature*, 521(7550), 65-69. [CrossRef]
- [18] He, Z., Wu, W., Wang, J., Ding, L., Chang, Q., & Huang, Y. (2024). Investigations into motion responses of suspended submersible in internal solitary wave field. *Journal of Marine Science and Engineering*, 12(4), 596. [CrossRef]
- [19] Yue, H., Zhang, H., Zhu, Q., Ai, Y., Tang, H., & Zhou, L. (2025). Wake dynamics of a wind turbine under real-time varying inflow turbulence: A coherence mode perspective. *Energy Conversion and Management*, 332, 119729. [CrossRef]
- [20] Bernitsas, M. M., Raghavan, K., Ben-Simon, Y., & Garcia, E. M. H. (2008). VIVACE (Vortex Induced Vibration Aquatic Clean Energy): A New Concept in Generation of Clean and Renewable Energy From Fluid Flow. *Journal of Offshore Mechanics and Arctic Engineering*, 130(4), 041101. [CrossRef]
- [21] Frahm, H. (1911). *U.S. Patent No. 989,958*. Washington, DC: U.S. Patent and Trademark Office.
- [22] Den Hartog, J. P. (1985). *Mechanical vibrations*. Courier Corporation.
- [23] Poon, D., Shieh, S. S., Joseph, L. M., & Chang, C. (2004, October). Structural design of Taipei 101, the world's tallest building. In *Proceedings of the ctbuh 2004 seoul conference, seoul, korea* (pp. 271-278). sn.
- [24] Lee, Y. S., Kerschen, G., McFarland, D. M., Hill, W. J., Nickkawde, C., Strganac, T. W., ... & Vakakis, A. F. (2007). Suppressing aeroelastic instability using broadband passive targeted energy transfers, part 2: experiments. *AIAA journal*, 45(10), 2391-2400. [CrossRef]
- [25] Chao, C., Dai, W., Shi, B., Branson, D., & Yang, J. (2025). Suppression of self-excited vibrations using tuned mass damper or nonlinear energy sink. *Nonlinear Dynamics*, 113(23), 32007-32035. [CrossRef]
- [26] Yang, F., Sedaghati, R., & Esmailzadeh, E. (2022). Vibration suppression of structures using tuned mass damper technology: A state-of-the-art review. *Journal of Vibration and Control*, 28(7-8), 812-836. [CrossRef]
- [27] Mehmood, A., Nayfeh, A. H., & Hajj, M. R. (2014). Effects of a non-linear energy sink (NES) on vortex-induced vibrations of a circular cylinder. *Nonlinear dynamics*, 77(3), 667-680. [CrossRef]
- [28] VAKAKIS, A. (2001). Inducing passive nonlinear

- energy sinks in vibrating systems. *Journal of vibration and acoustics*, 123(3), 324-332. [CrossRef]
- [29] Daqaq, M. F., Masana, R., Erturk, A., & Dane Quinn, D. (2014). On the role of nonlinearities in vibratory energy harvesting: a critical review and discussion. *Applied mechanics reviews*, 66(4), 040801. [CrossRef]
- [30] Kang, X., Huang, Q., Wu, Z., Tang, J., Jiang, X., & Lei, S. (2024). A Review of the Tuned Mass Damper Inerter (TMDI) in Energy Harvesting and Vibration Control: Designs, Analysis and Applications. *Computer Modeling in Engineering & Sciences (CMES)*, 139(3). [CrossRef]
- [31] Warburton, G. B. (1982). Optimum absorber parameters for various combinations of response and excitation parameters. *Earthquake engineering & structural dynamics*, 10(3), 381-401. [CrossRef]
- [32] Zhang, Z., Lu, Z. Q., Ding, H., & Chen, L. Q. (2019). An inertial nonlinear energy sink. *Journal of Sound and Vibration*, 450, 199-213. [CrossRef]
- [33] Guilmineau, E., & Queutey, P. (2004). Numerical simulation of vortex-induced vibration of a circular cylinder with low mass-damping in a turbulent flow. *Journal of fluids and structures*, 19(4), 449-466. [CrossRef]
- [34] Qi, X. K., Zhang, J. C., Wang, J., & Li, B. Q. (2024). Research on vibration suppression of nonlinear energy sink with linear damping and geometrically nonlinear damping. *Nonlinear Dynamics*, 112(15), 12721-12750. [CrossRef]
- [35] Jing, X. J., & Lang, Z. Q. (2009). Frequency domain analysis of a dimensionless cubic nonlinear damping system subject to harmonic input. *Nonlinear Dynamics*, 58(3), 469-485. [CrossRef]
- [36] Al-Shudeifat, M. A. (2017). Nonlinear energy sinks with nontraditional kinds of nonlinear restoring forces. *Journal of Vibration and Acoustics*, 139(2), 024503. [CrossRef]
- [37] Saeed, A. S., AL-Shudeifat, M. A., & Vakakis, A. F. (2019). Rotary-oscillatory nonlinear energy sink of robust performance. *International Journal of Non-Linear Mechanics*, 117, 103249. [CrossRef]
- [38] Saeed, A. S., AL-Shudeifat, M. A., Vakakis, A. F., & Cantwell, W. J. (2020). Rotary-impact nonlinear energy sink for shock mitigation: analytical and numerical investigations. *Archive of Applied Mechanics*, 90(3), 495-521. [CrossRef]
- [39] Gendelman, O. V., & Alloni, A. (2015). Dynamics of forced system with vibro-impact energy sink. *Journal of Sound and Vibration*, 358, 301-314. [CrossRef]
- [40] AL-Shudeifat, M. A., & Nasar, R. A. (2025). On rapid vibration suppression by nonlinear energy sink during first half cycle of oscillation. *Communications in Nonlinear Science and Numerical Simulation*, 142, 108534. [CrossRef]
- [41] Gourdon, E., Alexander, N. A., Taylor, C. A., Lamarque, C. H., & Pernot, S. (2007). Nonlinear energy pumping under transient forcing with strongly nonlinear coupling: Theoretical and experimental results. *Journal of sound and vibration*, 300(3-5), 522-551. [CrossRef]
- [42] Huang, X., & Zhong, T. (2023). Hydrokinetic energy harvesting from flow-induced vibration of a hollow cylinder attached with a bi-stable energy harvester. *Energy Conversion and Management*, 278, 116718. [CrossRef]
- [43] Facchinetti, M. L., De Langre, E., & Biolley, F. (2004). Coupling of structure and wake oscillators in vortex-induced vibrations. *Journal of Fluids and structures*, 19(2), 123-140. [CrossRef]
- [44] Cottone, F., Vocca, H., & Gammaitoni, L. (2009). Nonlinear energy harvesting. *Physical review letters*, 102(8), 080601. [CrossRef]
- [45] Harne, R. L., & Wang, K. W. (2013). A review of the recent research on vibration energy harvesting via bistable systems. *Smart materials and structures*, 22(2), 023001. [CrossRef]
- [46] Yurchenko, D., Lai, Z. H., Thomson, G., Val, D. V., & Bobryk, R. V. (2017). Parametric study of a novel vibro-impact energy harvesting system with dielectric elastomer. *Applied energy*, 208, 456-470. [CrossRef]
- [47] Wu, Y., & Wu, H. (2025). A novel flow-induced motion energy harvesting with coupled mechanism of time-varying stiffness and passive turbulence control. *Physics of Fluids*, 37(6). [CrossRef]
- [48] Mazzolai, B., Laschi, C., Cianchetti, M., Patane, F., Bassi-Luciani, L., Izzo, I., & Dario, P. (2007, August). Biorobotic investigation on the muscle structure of an octopus tentacle. In *2007 29th Annual International Conference of the IEEE Engineering in Medicine and Biology Society* (pp. 1471-1474). IEEE. [CrossRef]
- [49] Wu, H., Wu, Y., & Jia, S. (2023). The performance investigation of flow-induced motion energy-harvesting by applying time-varying stiffness in the dynamic ocean environment. *Ocean Engineering*, 286, 115618. [CrossRef]
- [50] Smith, M. C. (2002). Synthesis of mechanical networks: the inerter. *IEEE Transactions on automatic control*, 47(10), 1648-1662. [CrossRef]
- [51] Zhang, W., Zhang, W., & Guo, X. (2023). Vertical vibration control using nonlinear energy sink with inertial amplifier. *Applied Mathematics and Mechanics*, 44(10), 1721-1738. [CrossRef]
- [52] Lu, Z. Q., Ding, H., & Chen, L. Q. (2019). Resonance response interaction without internal resonance in vibratory energy harvesting. *Mechanical Systems and Signal Processing*, 121, 767-776. [CrossRef]
- [53] Wang, J., Zhou, S., Zhang, Z., & Yurchenko, D. (2019). High-performance piezoelectric wind energy harvester with Y-shaped attachments. *Energy conversion and management*, 181, 645-652. [CrossRef]

- [54] Wang, J., Geng, L., Ding, L., Zhu, H., & Yurchenko, D. (2020). The state-of-the-art review on energy harvesting from flow-induced vibrations. *Applied Energy*, 267, 114902. [CrossRef]
- [55] Wang, J., Gu, S., Zhang, C., Hu, G., Chen, G., Yang, K., ... & Yurchenko, D. (2020). Hybrid wind energy scavenging by coupling vortex-induced vibrations and galloping. *Energy Conversion and Management*, 213, 112835. [CrossRef]
- [56] Chang, C. C. J., Kumar, R. A., & Bernitsas, M. M. (2011). VIV and galloping of single circular cylinder with surface roughness at $3.0 \times 10^4 \leq Re \leq 1.2 \times 10^5$. *Ocean Engineering*, 38(16), 1713-1732. [CrossRef]
- [57] Hu, G., Tse, K. T., Wei, M., Naseer, R., Abdelkefi, A., & Kwok, K. C. (2018). Experimental investigation on the efficiency of circular cylinder-based wind energy harvester with different rod-shaped attachments. *Applied energy*, 226, 682-689. [CrossRef]
- [58] Park, H., Bernitsas, M. M., & Chang, C. C. (2013, June). Map of passive turbulence control to flow-induced motions for a circular cylinder at $30,000 < re < 120,000$: sensitivity to zone covering. In *International Conference on Offshore Mechanics and Arctic Engineering* (Vol. 55416, p. V007T08A003). American Society of Mechanical Engineers. [CrossRef]
- [59] Ding, L., Mao, X., Yang, L., Yan, B., Wang, J., & Zhang, L. (2021). Effects of installation position of fin-shaped rods on wind-induced vibration and energy harvesting of aeroelastic energy converter. *Smart Materials and Structures*, 30(2), 025026. [CrossRef]
- [60] Sun, H., Yang, Z., Li, J., Ding, H., & Lv, P. (2024). Performance evaluation and optimal design for passive turbulence control-based hydrokinetic energy harvester using EWM-based TOPSIS. *Energy*, 298, 131377. [CrossRef]
- [61] Betz, A. (2014). *Introduction to the Theory of Flow Machines*. Elsevier.
- [62] Tamimi, V., Esfehiani, M. J., Zeinoddini, M., Naeeni, S. T. O., Wu, J., & Shahvaghari-Asl, S. (2020). Marine hydrokinetic energy harvesting performance of diamond and square oscillators in tandem arrangements. *Energy*, 202, 117749. [CrossRef]
- [63] Zhu, H., Zhao, Y., & Zhou, T. (2018). CFD analysis of energy harvesting from flow induced vibration of a circular cylinder with an attached free-to-rotate pentagram impeller. *Applied energy*, 212, 304-321. [CrossRef]
- [64] Park, H., Kumar, R. A., & Bernitsas, M. M. (2013). Enhancement of flow-induced motion of rigid circular cylinder on springs by localized surface roughness at $3 \times 10^4 \leq Re \leq 1.2 \times 10^5$. *Ocean Engineering*, 72, 403-415. [CrossRef]
- [65] Li, N., Park, H., Sun, H., & Bernitsas, M. M. (2022). Hydrokinetic energy conversion using flow induced oscillations of single-cylinder with large passive turbulence control. *Applied Energy*, 308, 118380. [CrossRef]
- [66] Park, H., Mentzelopoulos, A. P., & Bernitsas, M. M. (2023). Hydrokinetic energy harvesting from slow currents using flow-induced oscillations. *Renewable Energy*, 214, 242-254. [CrossRef]
- [67] Chen, W. L., Gao, D. L., Yuan, W. Y., Li, H., & Hu, H. (2015). Passive jet control of flow around a circular cylinder. *Experiments in Fluids*, 56(11), 201. [CrossRef]
- [68] Wang, J., Han, C., Yurchenko, D., Zhou, Y., Meng, X., & Zhang, W. (2024). Energy concentration pipe based on passive jet control for enhancing flow induced vibration energy harvesting. *Energy Conversion and Management*, 319, 118948. [CrossRef]
- [69] Wang, X. J., Chen, W. L., Gao, D. L., Yang, W. H., & Li, H. (2020). Passive jet approach to control the flow over a circular cylinder. *Journal of Aerospace Engineering*, 33(3), 04020015. [CrossRef]
- [70] Xu, F., Chen, W. L., Duan, Z. D., & Ou, J. P. (2020). Large eddy simulation of passive jet flow control on the wake of flow around a circular cylinder. *Computers & Fluids*, 196, 104342. [CrossRef]
- [71] Huang, Z., Wang, J., Zhang, D., & Wang, X. (2025). Investigation of vibration suppression by nonlinear energy sink (NES) based on structure-wake oscillator coupled model. *International Journal of Non-Linear Mechanics*, 105219. [CrossRef]
- [72] Bearman, P. W., Gartshore, I. S., Maull, D. J., & Parkinson, G. V. (1987). Experiments on flow-induced vibration of a square-section cylinder. *Journal of Fluids and Structures*, 1(1), 19-34. [CrossRef]
- [73] Wang, J., Tang, B., Yang, H., Zhu, G., & Tan, W. (2025). Energy harvesting of flow induced vibration enhanced by bionic non-smooth surfaces. *Chinese Journal of Mechanical Engineering*, 38(1), 79. [CrossRef]
- [74] Sun, W., Wang, Y., Liu, Y., Su, B., Guo, T., Cheng, G., ... & Seok, J. (2024). Navigating the future of flow-induced vibration-based piezoelectric energy harvesting. *Renewable and Sustainable Energy Reviews*, 201, 114624. [CrossRef]
- [75] Williamson, C. H. K., & Govardhan, R. (2004). Vortex-Induced Vibrations. *Annual Review of Fluid Mechanics*, 36, 413-455. [CrossRef]
- [76] Nguyen, V. T., & Nguyen, H. H. (2016). Detached eddy simulations of flow induced vibrations of circular cylinders at high Reynolds numbers. *Journal of Fluids and Structures*, 63, 103-119. [CrossRef]